27 June 1997

ELSEVIER

Chemical Physics Letters 272 (1997) 245–249

CHEMICAL PHYSICS LETTERS

# SQUID detected NMR of laser-polarized xenon at 4.2 K and at frequencies down to 200 Hz

Dinh M. TonThat [a], M. Ziegeweid [b], Y.-Q. Song [b], E.J. Munson [b,1], S. Appelt [b,2], A. Pines [b], John Clarke [a]

[a] *Materials Sciences Division, Lawrence Berkeley National Laboratory and Department of Physics, University of California, Berkeley, CA 94720, USA*

[b] *Materials Sciences Division, Lawrence Berkeley National Laboratory and Department of Chemistry, University of California, Berkeley, CA 94720, USA*

Received 28 October 1996; in final form 22 April 1997

**Abstract**

A spectrometer based on a dc SQUID (superconducting quantum interference device) was used to record nuclear magnetic resonance signals from laser-polarized $^{129}Xe$ at 4.2 K and at frequencies ranging from about 200 Hz to 110 kHz in magnetic fields varying from about 0.02 to 9 mT. The $^{129}Xe$ resonance linewidths were found to increase with increasing magnetic field, and, at a given field, to increase with higher $^{129}Xe$ concentration. The spin-lattice relaxation times were observed to decrease from $\sim 8000$ s at 5 mT to $\sim 2000$ s at fields below 0.05 mT. Such long relaxation times make possible a variety of spin polarization transfer experiments. © 1997 Published by Elsevier Science B.V.

By means of optical pumping with circularly polarized laser light and through the intermediary of alkali metal vapor, the nuclear spin polarization of gaseous xenon can be increased by up to five orders of magnitude with respect to the Boltzmann polarization at room temperature and 4 tesla [1–3]. The enhancement in nuclear magnetic resonance (NMR) signal by this "hyperpolarization" has made possible a number of novel experiments, among them enhanced magnetic resonance imaging (MRI) of organisms [4–8] and enhanced NMR of surfaces and solutions [9–11]. In view of its function as an NMR/MRI contrast agent, a spin-polarization source for cross polarization [12–14], and a potential low-temperature NMR/NQR matrix [15], previous investigations have addressed the question of the relaxation of xenon in gas [16], solution [17], and solid phases [18–20]. Of particular relevance for the long term storage of hyperpolarized xenon at low temperatures is the decay of the polarization via spin-lattice relaxation as the magnetic field is reduced towards zero. Gatzke et al. [20] reported the $^{129}Xe$ spin-lattice relaxation time, $T_1$, at 4.2K in magnetic fields ranging from 0.2 T to 5 mT, corresponding to $^{129}Xe$ Larmor frequencies of 2 MHz to 50 kHz. They found that $T_1$ depends strongly on magnetic field in this range.

[1] Present address: Department of Chemistry, University of Minnesota, 207 Pleasant St. SE, Minneapolis, MN 55455, USA.

[2] Present address: Department of Physics, Princeton University, Princeton, NJ 08544, USA.


*PII* S0009-2614(97)00514-9

At yet lower magnetic fields and correspondingly lower NMR frequencies, the detection of NMR signals by conventional tuned circuits becomes difficult because the signal-to-noise ratio decreases, quadratically for equilibrium spin polarizations and linearly for the laser polarized case, as the NMR frequency is lowered. For gaseous xenon, optical detection is possible at low fields [21–23], but is precluded for low-temperature solids. To overcome such difficulties, we previously constructed an NMR spectrometer based on a dc SQUID (superconducting quantum interference device) [24] to detect precessing nuclear moments, and used it to observe NQR of $^{27}$Al and $^{14}$N at frequencies as low as 17 kHz [25–27]. The SQUID, a flux-to-voltage transducer, detects magnetic flux rather than its time derivative and thus does not lose sensitivity at low frequencies [28].

In this Letter, we describe the use of the SQUID spectrometer to observe NMR signals from laser-polarized solid xenon at 4.2 K. This detection scheme enables us to extend the measurement of $T_1$ of solid xenon to very low magnetic fields, from 9 mT down to near zero. We find that $T_1$ continues to decrease at fields down to about 2 mT, below which it saturates at about 2000 s, thus ensuring the viability of xenon as a low-temperature, low-field source of spin polarization, in particular for surface and matrix studies.

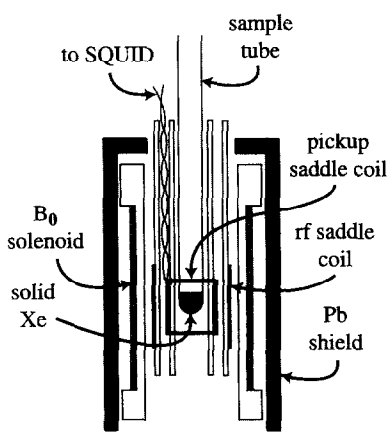


Fig. 1. Schematic drawing of the SQUID-based NMR spectrometer. The sample is at the center of the orthogonal pickup and excitation saddle coils; persistent current solenoid provides a static magnetic field along the axis of the sample tube. Coils and sample are enclosed in a Pb tube. Two $\mu$-metal shields (not shown) reduce the ambient magnetic field to below 0.1 $\mu$T.

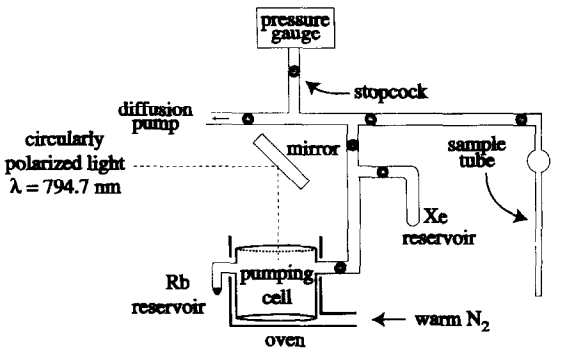


Fig. 2. Optical pumping apparatus, consisting of a 10 cm$^3$ cylindrical glass cell surrounded by a solenoid (not shown), a Rb reservoir, a xenon reservoir, and a sample cell linked by glass vacuum lines provided with stopcocks. The laser light illuminates the pumping cell via a circular polarizer.

Fig. 1 shows schematically the low-temperature part of the spectrometer; a detailed description appears elsewhere [27]. The signal is detected by a saddle coil, with two turns on each side, that is connected to the 50-turn input coil of the SQUID. This input circuit is entirely superconducting, and thus responds to magnetic flux at frequencies down to zero. A second saddle coil to provide radio frequency (rf) excitation is mounted orthogonally to the pickup coil. A superconducting solenoid with a thermal switch enabling it to be operated in a persistent current mode provides a static field $B_0$ perpendicular to the axes of the saddle coils. The coils are enclosed in a lead shield and the entire assembly is immersed in liquid $^4$He. The cryostat is surrounded with two $\mu$-metal shields to reduce the ambient magnetic field to below 0.1 $\mu$T. The tube containing spin-polarized xenon is inserted into the center of the coils.

The optical pumping apparatus is shown in Fig. 2. The pumping cell, a glass cylinder with a volume of 10 cm$^3$, is connected to the sample tube through glass transfer lines with stopcocks for gas handling. The cell is coated with a thin film of rubidium and heated by flowing nitrogen gas to 70–90°C to increase the rubidium vapor pressure for optimal absorption. During optical pumping, the cell is illuminated with a circularly polarized light from a 0.5 W cw tunable diode laser (Spectra Diode Laboratories). The laser is tuned to the rubidium D1 optical transition, 794.7 nm, and the fluorescence in the cell is monitored with an infrared viewer. Typically, we

load 2 mM of xenon into the pumping cell and irradiate it for 30 minutes. A magnetic field of 3 mT splits the Rb and Xe levels during optical pumping. Subsequently, we cool the cell to below 40°C to lower the rubidium vapor pressure, and allow the xenon gas to flow into the sample tube. The xenon freezes at the tip of this tube, which is immersed in liquid nitrogen, in the presence of a 0.1 T magnetic field. Finally, we insert the sample tube into the SQUID spectrometer. A solenoid around the top of the cryostat maintains the Xe in a 10 mT magnetic field during the transfer process, except for an interval of less than 1 s when the tube is lowered into the coils. We used both isotopically enriched xenon (80% $^{129}$Xe, 2% $^{131}$Xe, EG&G Mound) and naturally abundant xenon (26.4% $^{129}$Xe, 21.2% $^{131}$Xe); from separate, high-field experiments we estimate the enhanced polarization of the $^{129}$Xe to be 10%.

Fig. 3 shows six $^{129}$Xe NMR spectra obtained at fields ranging from 8.9 mT down to 0.019 mT with corresponding $^{129}$Xe Larmor frequencies of about 110 kHz to 200 Hz. These spectra were acquired

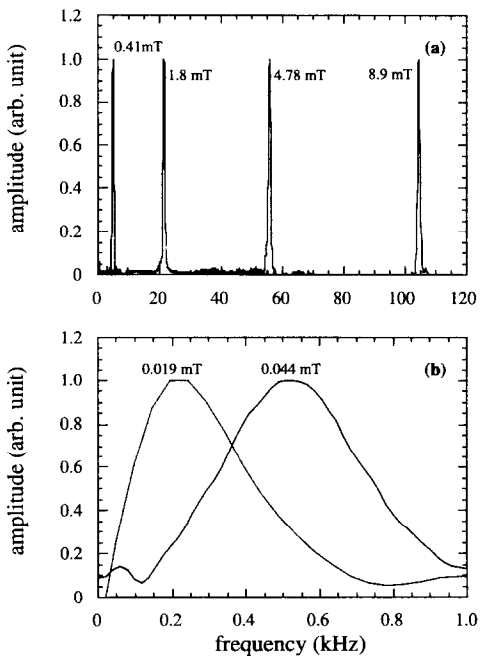


Fig. 3. SQUID-detected $^{129}$Xe NMR spectra from (a) isotopically enriched $^{129}$Xe (80%) at different 4 magnetic fields, and (b) isotopically enriched sample at 0.044 mT and naturally abundant sample at 0.019 mT.

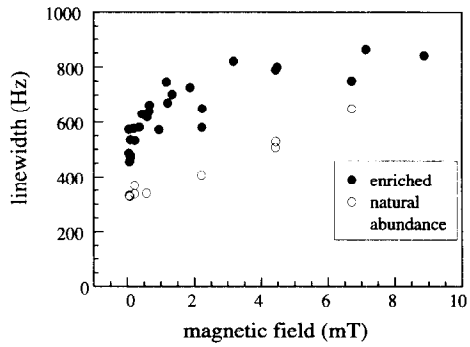


Fig. 4. The FWHM (full-width at half-maximum) of the $^{129}$Xe NMR spectra versus magnetic field, from 0.02 mT to 9 mT. At the lowest field, the FWHM is $520 \pm 60$ Hz and $340 \pm 20$ Hz for the isotopically enriched and naturally abundant samples, respectively.

with a single rf excitation pulse with a tipping angle of 8° for Fig. 3(a) and of 90° for Fig. 3(b). As shown in Fig. 4, the linewidth increases with increasing magnetic field for both the naturally abundant samples and the isotopically enriched samples. As the magnetic field is reduced to near zero, the FWHM (full-width at half-maximum) approaches $520 \pm 60$ Hz for the isotopically enriched samples and $340 \pm 20$ Hz for the naturally abundant samples. These values agree well with the 616 and 350 Hz linewidths calculated for nuclear dipolar interactions for the isotopically enriched and naturally abundant samples, respectively [29]. The increase in the linewidths at higher magnetic fields is largely due to the inhomogeneity of the solenoid, about 1%. From the signal-to-noise ratio of our data, assuming a $^{129}$Xe polarization of 10%, we estimate that at 20 kHz our spectrometer can detect approximately $5 \times 10^{15}$ $^{129}$Xe spins in a single shot.

The $T_1$ values are determined by measuring a series of $^{129}$Xe signals at different times after the sample is inserted into the spectrometer. For each measurement, a small rf excitation pulse is used with a tipping angle between 5° and 10°. We determine the tipping angles in a separate experiment by applying 20 pulses in rapid succession and measuring the resulting decay of the signal. The tipping angle is taken into account in evaluating $T_1$.

The decay of the xenon magnetization at most magnetic field values does not follow a single exponential function, indicating inhomogeneity in the re-

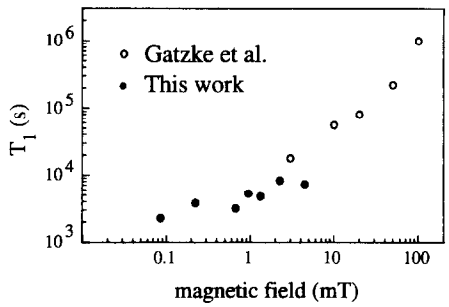


Fig. 5. $T_1$ for isotopically enriched (solid circles) $^{129}$Xe versus magnetic field; as well as the data by Gatzke et al. [20] at higher magnetic field (open circles). As the magnetic field approaches zero, $T_1$ tends towards a value of about 2000 s.

laxation process. We determine the $T_1$ from the initial decay of the signal, so that the quoted values are averaged over the distribution of the relaxation processes involved. Fig. 5 shows $T_1$ vs. magnetic field for the enriched sample measured at 4.2 K. The data of Gatzke et al. [20] over the magnetic field range 5 to 100 mT are also indicated in Fig. 5. We note that the value of $T_1$ obtained at the highest field in the current work is a factor of 2 or 3 lower than in the earlier work; we return to this point later. Despite this discrepancy, we see that $T_1$ is strongly dependent on magnetic field above a few mT and relatively insensitive to magnetic field below 2 mT. As the magnetic field approaches zero, $T_1$ saturates at approximately 2000 s.

We now turn to a brief discussion of the magnetic field dependence of $T_1$. Gatzke et al. [20] argue that at temperatures below 20 K the $^{129}$Xe relaxation arises primarily from cross-relaxation to $^{131}$Xe via the nuclear dipole interaction; because of their quadrupole moment, the $^{131}$Xe nuclei couple to the lattice more effectively than $^{129}$Xe. The effectiveness of this cross-relaxation depends on the overlap of the $^{129}$Xe and $^{131}$Xe resonance lines. The fact that the measured $T_1$ for the $^{129}$Xe nuclei is almost independent of magnetic field below 2 mT indicates that the $^{131}$Xe linewidth is very broad, about 20 kHz. This width, however, cannot be explained by dipolar broadening; the dipolar coupling of $^{131}$Xe is actually weaker than that of $^{129}$Xe because of the smaller gyromagnetic ratio of $^{131}$Xe and the lower $^{131}$Xe concentration in our sample. If the coupling of the $^{131}$Xe nuclei to the electric field gradient is neglected, the $^{129}$Xe and $^{131}$Xe lines will not overlap until the magnetic field is decreased below 0.025 mT (616 Hz/$2\gamma_{129}$) and 0.015 mT (350 Hz/$2\gamma_{129}$) for the enriched and the naturally abundant samples, respectively. These fields are lower than those in any of our experiments, implying that another mechanism, namely nuclear quadrupole coupling to the lattice, is responsible for broadening the $^{131}$Xe linewidth. Warren and Norberg [19] measured the linewidth of the naturally abundant $^{131}$Xe at 4.2 K in a magnetic field of 860 mT to be $2.4 \pm 0.2$ kHz, a value still too low to account for the saturation of $T_1$ in our experiments. We can explain this discrepancy as follows. In the direct detection of NMR in $^{131}$Xe, most of the nuclei contribute to the signal and the linewidth is dominated by nuclei in the bulk rather than on the surface or at grain boundaries [20]. We believe that the opposite situation prevails in the observation of the spin-lattice relaxation of $^{129}$Xe via cross-relaxation with $^{131}$Xe. In our case, the $^{131}$Xe nuclei in the bulk, with a linewidth of about 2.4 kHz, do not participate in the cross-relaxation until the magnetic field is below 0.7 mT. Thus at higher fields, the observed magnetic field dependence of $T_1$ for the $^{129}$Xe nuclei suggests that only those $^{131}$Xe nuclei near grain boundaries and defects, where the higher electric field gradients produce broader resonance linewidths, contribute to the cross-relaxation. Since the grain size depends on the details of the sample preparation, which is difficult to control, the fact that relaxation is dominated by nuclear quadrupole interactions at grain boundaries may well explain why our value of $T_1$ at about 4.5 mT is lower than that of Gatzke et al. [20].

In summary, the use of a dc SQUID to observe NMR of optically polarized $^{129}$Xe enables us to measure the magnetic field dependence of the spin-lattice relaxation time at much lower frequencies, approaching the xenon–xenon dipolar coupling energy, than have previously been attainable. At 4.2 K, the magnetization persists for sufficiently long times – more than 2000 s at 0.1 mT – to make possible a variety of cross-polarization experiments, for example, the transfer of polarization to surface or matrix isolated species. Since the spin-lattice relaxation time for many nuclei becomes very long at liquid $^4$He temperatures, the range of samples that can be studied by conventional signal averaging methods is

limited. The use of highly polarized xenon to enhance the polarization of such nuclei and thus avoid the necessity to signal average could enable one to perform measurements, including zero-field NMR and NQR [30–32], over a range of very low frequencies.

## Acknowledgements

We acknowledge the use of the Microelectronics Facility in the Electronics Research Laboratory of the Electrical Engineering and Computer Science Department, UC Berkeley. YQS was supported by a fellowship from the Miller Institute for Basic Research in Science. This work was supported by the Office of Energy Research, Office of Basic Energy Sciences, Materials Sciences Division, US Department of Energy under Contract No. DE-AC0376SF0098.

## References

[1] A. Kastler, J. Phys. Radium 11 (1950) 255.
[2] T.R. Carver, Science 141 (1963) 599.
[3] W. Happer, Rev. Mod. Phys. 44 (1972) 169.
[4] M.S. Albert, G.D. Cates, B. Driehuys, W. Happer, B. Saam, C.S. Springer Jr., A. Wishnia, Nature 370 (1994) 199.
[5] H. Middleton, R.D. Black, B. Saam, G.D. Cates, G.P. Cofer, R. Guenther, W. Happer, L.W. Hedlund, G.A. Johnson, K. Juvan, J. Swartz, J. Magn. Reson. Med. 33 (1995) 271.
[6] M. Leduc, E. Otten, La Recherche 287 (1996) 41.
[7] K. Sakai, A.M. Milek, E. Oteiza, R.L. Walsworth, D. Balamore, F. Jolesz, M.S. Albert, J. Mag. Res. B 111 (1996) 300.
[8] R.R. Swanson, M. Rosen, J.W. Stokes, P. Downing, Anaesth. Intensive Care (1996) (preprint).
[9] G. Navon, Y.-Q. Song, T. Room, S. Appelt, R.E. Taylor, A. Pines, Science 271 (1996) 1848.
[10] A. Bifone, Y.-Q. Song, R. Seydoux, R.E. Taylor, B.M. Goodson, T. Pietraß, T. Budinger, G. Navon, A. Pines, Proc. Natl. Acad. Sci. USA (1996) (accepted).
[11] T. Room, S. Appelt, R. Seydoux, E.L. Hahn, A. Pines, Phys. Rev. B (submitted).
[12] D. Raftery, H. Long, T. Meersman, P.J. Grandinetti, L. Reven, A. Pines, Phys. Rev. Lett. 66 (1991) 584.
[13] C.R. Bowers, H.W. Long, T. Pietraß, H.C. Gaede, A. Pines, Chem. Phys. Lett. 205 (1993) 168.
[14] H.C. Gaede, Y.-Q. Song, R.E. Taylor, E.J. Munson, J.A. Reimer, A. Pines, Appl. Mag. Res. 8 (1995) 373.
[15] K.W. Zilm, D.M. Grant, J. Am. Chem. Soc. 103 (1981) 2913.
[16] R.L. Streever, H.Y. Carr, Phys. Rev. 121 (1961) 20.
[17] K. Oikarinen, J. Jokisaari, Appl. Mag. Res. 8 (1995) 587.
[18] W.M. Yen, R.E. Norberg, Phys. Rev. 131 (1963) 269.
[19] W.W. Warren Jr., R.E. Norberg, Phys. Rev. 154 (1967) 277.
[20] M. Gatzke, G.D. Cates, B. Driehuys, D. Fox, W. Happer, B. Saam, Phys. Rev. Lett. 70 (1993) 690.
[21] T.M. Kwon, J.G. Mark, C.H. Volk, Phys. Rev. A 24 (1981) 1894.
[22] Z. Wu, W. Happer, J. Daniels, Phys. Rev. Lett. 59 (1987) 1480.
[23] D. Raftery, H.W. Long, D. Shykind, P.J. Grandinetti, A. Pines, Phys. Rev. A 50 (1994) 567.
[24] J. Clarke, in: The new superconducting electronics, eds. H. Weinstock, R.W. Ralston (Kluwer, Dordrecht, 1993) p. 123.
[25] N.Q. Fan, J. Clarke, Rev. Sci. Instrum. 62 (1991) 1453.
[26] M.D. Hurlimann, C.H. Pennington, N.Q. Fan, J. Clarke, Phys. Rev. Lett. 69 (1992) 684.
[27] Dinh M. TonThat, J. Clarke, Rev. Sci. Instrum. 67 (1996) 2890.
[28] J. Clarke, Z. Naturforsch. 49a (1994) 5.
[29] A. Abragam, The principles of nuclear magnetism (Clarendon, Oxford, 1989).
[30] A. Bielecki, D.B. Zax, K.W. Zilm, A. Pines, Rev. Sci. Instrum. 57 (1986) 393.
[31] J.M. Millar, A.M. Thayer, A. Bielecki, D.B. Zax, A. Pines, J. Chem. Phys. 83 (1985) 934.
[32] D.B. Zax, A. Bielecki, K. Zilm, A. Pines, D.P. Weitekamp, J. Chem. Phys. 83 (1985) 4877.